Structural Changes of Circularly Defected Monolayer Circular Graphene Nanosheets Upon Mechanical Vibrations

M. Farzannasab[1], M. M. Khatibi[1,*] and S. Sadeghzadeh[2]

[1]*Modal Analysis (MA) Research Laboratory, Faculty of Mechanical Engineering, Semnan University, Semnan, Iran*
[2]*Smart Micro/Nano Electro-Mechanical Systems Lab (MNEMS), School of New Technologies, Iran University of Science and Technology, Tehran, Iran*
E-mail: mmkhatibi@semnan.ac.ir
*Corresponding Author

Abstract

As the strongest and toughest material known, graphene has found numerous applications in various types of sensors. Due to the great influences of the graphene sheet's geometry on resonance frequency, circular defects could effect on expected results of sensors. Circular holes in circular graphene sheets (CGSs) have been modeled with molecular dynamics (MD) simulation in the present work. Then the vibration behavior of intact circular plate and circular sheet with the circular defect has been investigated using frequency-domain analysis (FDD). Furthermore, for validating the used method, the obtained natural frequencies for different graphene sheets have been compared with acquired data in former research. The result of validation showed the accuracy of the used method in this study. The results indicated that by increasing the hole size, the natural frequency of a defected sheet with free edges will be diminished, and with simply-supported interior boundary conditions typically went up. Also, by increasing the hole's eccentricity, the

natural frequency of the defected graphene sheet will be diminished when the hole boundary was subjected to simply-support or free condition.

1 Introduction

The discovery of graphene (carbon's allotrope) has opened a new horizon in developing automatic devices. Graphene is an extremely thin monolayer of carbon atoms in a hexagonal configuration and two-dimensional arrangement with extraordinary mechanical strength. Due to the high natural frequency of graphene, this material has gained a considerable reputation in different applications [1–4]. Graphene has great potential for electrical applications with a high frequency and can be utilized in various types of sensors due to its superior mechanical, thermal, and electrical properties [5–7]. The extensive use of graphene and other 2D materials in the fabrication of new sensors has made it necessary to conduct serious studies on increasing the frequency of these types of sensors [8–10]. Because of the CGSs properties, computer simulation can play a crucial role in future research works in this field. It is very important to review the former studies for validating the simulation results that have been conducted by employing numerical and theoretical approaches [10]. Murmur and Pradhan [11] used the non-local elasticity theory to study the vibration responses of single-layer CGSs. They demonstrated that the fundamental frequency of graphene monolayers was severely dependent on small-scale coefficients. Pradhan and Phadikar [12] analyzed the multilayer graphene sheet's vibration embedded in a polymer matrix and showed that the non-local effects on these sheets were substantial. Fazelzadeh and Pouresmaeeli [13] studied the effect of thermo-mechanical vibration on orthotropic nanoplates surrounded by an elastic medium. Several researchers have attempted to use molecular dynamics for studying the vibration behavior of CGSs. Arash et al. [14] used the non-local continuum theory to explore the free vibration of single and double-layer graphene. They then compared the results with those obtained by the molecular dynamics method. Also, the molecular dynamics method is used for studies based on continuum mechanics and, especially, the non-local theories [15–18] Neek-Amal and Peeters [19] have employed non-equilibrium molecular dynamics to investigate the buckling and hardness of circular monolayer graphene versus radial load. Recently, authors have presented valuable work on the

superiority of borophene compared to graphene in resonance [20]. They stated that a rectangular borophene sheet might have a higher natural frequency than a graphene resonator with the same mass. Jalali et al. [21] concluded that the circular hole size and diameter would significantly affect the stress concentration factor of single-layer CGSs. Mirakhory et al. [22] investigated vibration analysis of defected and pristine triangular single-layer graphene nanosheets Madani et al. [23] investigated the vibration behavior of annular CGS and the variation of geometry and inner-to-outer circle radiuses' ratio. They maintained that the natural frequencies of CGSs could be easily determined by applying the modified non-local theory. A review of published papers indicated that graphene is widely used in the industry, and mechanical nano-vibrators as one of the most important nano-electromechanical systems due to its high natural frequency (above GHz). As an example, CGSs can be used as thermal Nano-switches in electrical circuits that require very high accuracy. Another application of CGSs is in biomechanics which can point to cyclic nano-filters that trap and destroy cancer cells. On the other hand, graphene's exceptional thermal properties are used to enhance the strength and thermal conductivity of Nanostructures [7]. It may be possible that a pin was considered as a constraint on graphene monolayer sheets during the fabrication process of a nanostructure comprising CGSs. In this case, a porosity of different dimensions may be created for purposes such as vibration control, structural parameter identification and, damage detection. Some of these holes can be considered as a circular hole with the desired dimensions and location. Thus analyzing the behavior of circular CGSs with holes is an important affair. In this research, the vibration of CGSs with centric and eccentric holes through the MD method was studied and, obtained resonances for defected and pristine CGSs were compared with each other.

2 Theoretical Principles

2.1 Modelling Methods

As an atomic approach, MD is an accurate method in physics to simulate complex multi-particle systems. In this approach, the phase paths of systems comprising thousands of interacting particles are obtained by solving Hamilton's equations and applying appropriate boundary conditions. By analyzing the paths of particles in the phase space and using statistical mechanics, which are the intermediaries between microscopic and macroscopic quantities, different characteristics of a system, including its energy

and structural, dynamical, and mechanical properties, can be obtained. In molecular dynamics simulation, successive configurations of a system are obtained by integrating Newton's motion equations. The result of MD is a path that shows the positions or velocities of system particles versus time. The thermodynamic and time-dependent properties can be calculated using the approaches of molecular dynamics. The purpose of this article is to analyze the vibrations of homogeneous CGSs with a uniform thickness of 'h' in the cylindrical coordinates (r, θ, and z). In methods dealing with interatomic potentials and known as molecular dynamics methods, electrons were ignored. The energy of the system was expressed solely based on the location of the atoms' nuclei. Thus, the best way to model systems with high atom numbers is molecular dynamics methods [24]. Although this method accurately models the system's behavior with quantum mechanics in many cases, it cannot calculate the properties that depend on the location of the electrons.

In molecular dynamics and Monte Carlo methods, atoms and molecules' movement is based on the force exchanged between them. According to Newton's second law and the mass of carbon atoms, the acceleration and the displacement of atoms will be calculated in this study. The forces applied to each atom in an atomic system depend on the potential function of that system [24].

The potential function of an n-particle system describes how the potential energy of this system of particles depends on the atoms' location. The forces applied to each particle in molecular dynamics simulations are described in the Equation (1).

$$F_i = -\frac{\partial U(r_1, r_2, \ldots, r_N)}{\partial r_i} \tag{1}$$

When potential functions were used for molecular dynamics simulation, three advantages were obtained in simulation: simulations accurately, Transferability and Computational Speed [24].

The following methods could extract the potential function for a particular system,

- First method: Usually, A hypothetical form is considered for the potential function, and then the parameters are chosen to predict the results of the experiments. As an example, the parameters of a potential function are changed such that the melting temperature, evaporation energy, qualitative dynamic behaviors, etc. were obtained by molecular dynamics simulations correctly. The potential functions obtained by

this method are called potential empirical functions [25] (For example: Lennard-Jones, Morse, and Bourne-Meyer [26]).

- Second method: Direct use of quantum mechanic's electronic structure calculations to calculate forces in simulating molecular dynamics, such as the Car-Parrinello method [27].
- Third method: In this method, the electronic wave function [28] was calculated for the fixed location of the atoms. This method, is one of the most commonly used methods in LAMMPS software thus this method was used in this study [29].

It should be noticed that the purpose of using different potential models is not to achieve a specific property of matter but to change the arrangement of atoms. However, if the arrangement of substance changes due to the change in the interaction of atoms, some properties of the substance also change unintentionally.

The graphene lattice was modeled in a cubic box with periodic boundary conditions in all three Cartesian directions to avoid the effect of free atoms on edges. If the boundary of the box is periodic, so that particles interact across the boundary, and they can exit one end of the box and re-enter the other end. A periodic dimension can change in size due to constant pressure boundary conditions or box deformation. And if the boundary of the box is non-periodic, so that particles do not interact among the boundary and do not move from one side of the box to the other [33]. The sampling time in the simulation process was set to 0.1×10^{-15} s (0.1 femtosecond). An overall schematic of the procedure used in this study is depicted in Figure 1. Indeed Figure 1 present the communication among molecular dynamics and the frequency domain analysis method.

The dynamic behavior of the system is extracted using the molecular dynamics method. In molecular dynamics simulation, the official statistical mechanic's definitions for the ensembles are employed, so-called "ensemble". They mention the system variables that are arranged. In all ensembles, the number of particles (N) is conserved. The most significant ensembles are NVE, NVT, and NPT. In NVE, Simulation of a system based on constant-number (N), constant-volume (V), and constant-energy (E), the sum of kinetic (KE) and potential energy (PE) is conserved. And in NVT, Simulation of a system based on a constant number (N), constant-volume (V), and constant-temperature (T) [4, 33]. In order to model the small-scale system, the molecular dynamics simulation is carried out along with the LAMMPS software. the small-scale materials are classified into three categories that are
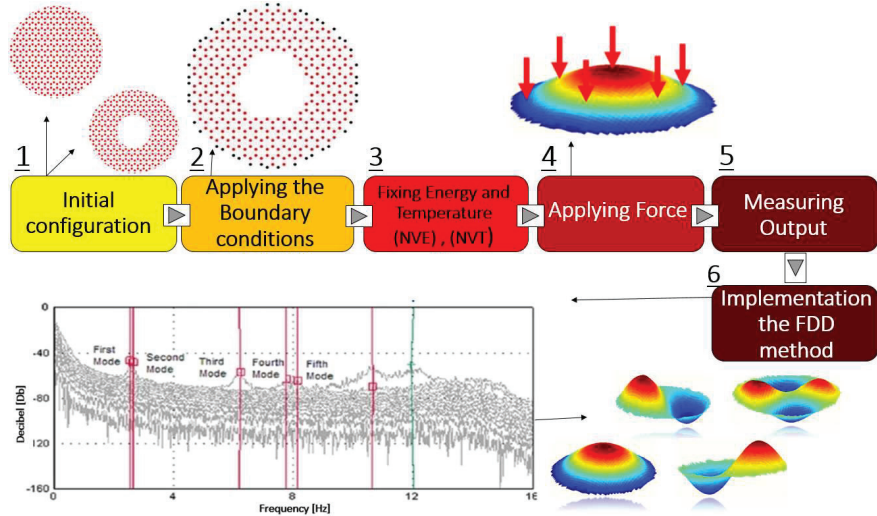
Figure 1 Molecular dynamics and frequency domain decomposition have been joined together to derive the free vibration behavior of 2D Nanostructure.

based on their dimensions: (i) thin films whose dimension in one direction is close to micrometers or less; (ii) thin wires/fibers whose dimensions in two directions are very small; and (iii) small particles [30, 31]. In the small-scale system, the structure is organized by the extremely aligned graphene Nano fillers and the polymer matrix. Afterwards, the structure phase and the porous area will be combined to form the large-scale system to illustrate the graphene nanocomposite foams [32, 12]. LAMMPS software is a molecular dynamics code that has a focus on materials modeling. This software various potentials assume for solid-state materials (metals, semiconductors) and soft matter (biomolecules, polymers), and coarse-grained or mesoscopic systems. It can be used to model atoms or, more generically, as an equal particle simulator at the atomic or continuum scale [33]. Figure 2 shows a circular sheet with a radius of R1 with a circular hole with a radius lattice of R2. Due to the great influence of geometry and boundary conditions on the sheet's frequency and the need for precise dimensions and sizes in the simulation, the outer circle has always been considered with a fixed radius. The boundary conditions were assumed to be simply supported to compare the natural frequencies of different holes (inner circle) conditions. Hence, the circular hole within the sheet has different dimensions, coordinates, and boundary conditions.

The graphene monolayer's geometry does not change during the simulation, and the radius of pristine sheets was considered 20 Å. Firstly, a
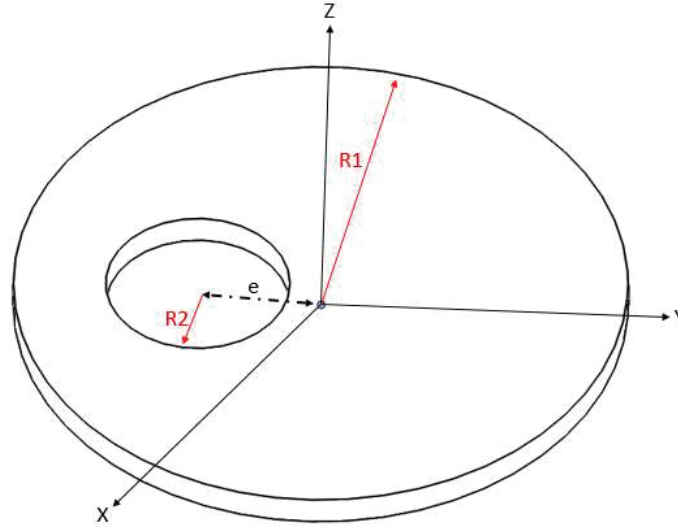
Figure 2   The geometry of a holed CGS with R1 as the radius of the sheet and R2 as the radius of the hole. The hole has an eccentricity equal to 'e'.

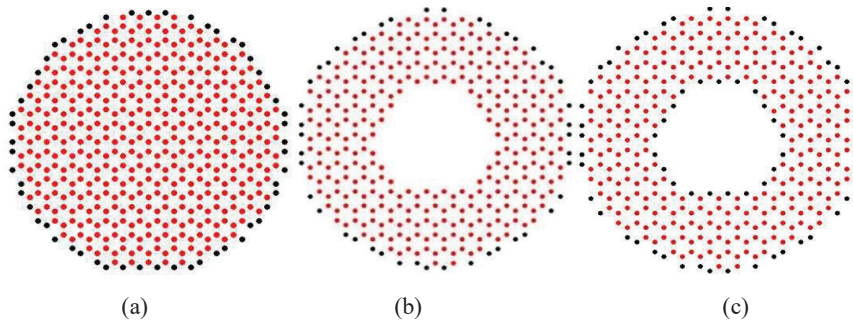(a)   (b)   (c)

Figure 3   (a) A defect-free CGS with SS boundary conditions, (b) FS boundary conditions for a CGS with a circular hole, (c) SS boundary conditions for a CGS with a circular hole.

simply-supported pristine graphene sheet and then a circularly defected circular sheet has been simulated. Fixed circular graphene has been considered for all the examined cases, and the simulation results have been tabulated in some tables and figures for comparison. As shown in Figure 3, Black atoms are those that are fixed on the plate to ensure boundary conditions. The boundary condition in applied to both outer and inner boundary atoms and one row of atoms at the boundaries is fixed to satisfy the simply-supported edge condition. This approach guarantees simply-supported boundary conditions [34].
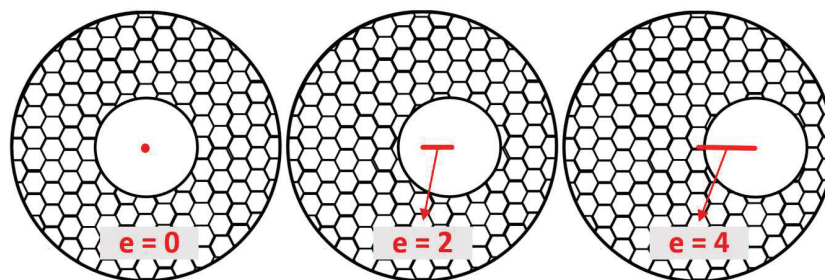
Figure 4   The geometry of different positions of the circular hole. The hole has an eccentricity equal to 'e'.

As shown in Figure 4, the circular hole's position is studied in three different situations that the distance of the center of the circular hole to the CGS was shown by "e".

First, an adequately large force was imposed on an arbitrary part of the CGS for a femtosecond duration, and then the applied force was removed, and the CGS is allowed to move with its natural dynamics. The dynamic response should be recorded in a relatively long-time-interval and include a large number of oscillations so that all frequencies of the system could be extracted. Due to the high operating frequency of CGSs and the non-dimensional form of molecular dynamics, a scaling analysis was essential. To calculation the system's frequency, the response of analysis parameters must be adjusted based on each atom's time-displacement signal. The initial parameter of the system was 'dt'. This parameter was usually determined by the stability of the molecular dynamics problem solving, and a parameter is already predefined, which was considered in the current problem of 0.1 fs. Based on the value of 'dt'; the maximum calculated frequency could be $1/2$ dt, which is about 5000 THz. The amount of scaled 'dt' was used $(dt = 0.01)$ for simplicity. Furthermore, in order to increase the accuracy of the computation, the original solving time (the time after the system arrives at the thermodynamic equilibrium) must be selected long enough to provide sufficient data for spectral analysis. Here, the total time is 5×10^6 the step that is equal to 0.5 ns. The dynamic fluctuations of some special atoms in the CGS were printed out time by time. The number of those special atoms and the order and distribution were very important and effective on the final results. Obtained displacement and the time could be used in the FDD approach to extract the natural frequencies and modes.

As observed in Figure 3, the two boundary conditions of FS and SS were evaluated as SS, where the inner and outer boundaries were both

simply-supported, and FS, where the internal boundary was free, and the outer boundary was simply-supported.

2.2 Derivation of Natural Frequencies and Mode Shapes Using FDD Method

In this paper, the frequencies and mode shapes have been derived by a handwritten code based on the FDD approach. The ambient modal analysis methods are categorized to parametric and non-parametric. In the parametric approach, a parametric model is approximated and adapted to the measured data in the time domain [35]. In the non-parametric model, the dynamic properties are extracted in the frequency domain, using some mathematical operations [36].

The frequency domain decomposition (FDD) is a non-parametric approach. In this method, the response of the power spectral density (PSD) of the structure is computed and then the singular value decomposition (SVD) technique is applied [37, 38]. The FDD method is based on the relationship between input and output [37]. Equation (2) shows the relationship between the input and output of the system.

$$G_{yy}(j\omega) = \overline{H}(j\omega) \cdot G_{xx}(j\omega) \cdot H^{T}(j\omega) \tag{2}$$

where $G_{xx}(j\omega)$ is the input power spectral density matrix, $G_{yy}(j\omega)$ is the output power spectral density matrix and $\overline{H}(j\omega)$ is the frequency response function matrix.

The power density of responses can be expressed in terms of the system mode shapes and poles, as Equation (3) [37].

$$G_{yy}(j\omega) = \sum_{k=1}^{n} \frac{d_k \varphi_k \varphi_k^t}{j\omega - \lambda_k} \frac{\overline{d}_k \overline{\varphi}_k \overline{\varphi}_k^t}{j\omega - \overline{\lambda}_k} \tag{3}$$

where, d_k is a scalar, φ_k is the kth mode shape and λ_k is the kth natural frequency.

Due to the Equation (3), at each frequency, a finite number of modes participate in create the response of the system. Close to the natural frequencies, only one mode contributes to system response. If, at each frequency, the response power spectral density matrix (Equation (2)) is decomposed into its singular values and vectors, since the singular values are directly related to the participation factors of modes, the number of non-zero singular values will demonstrate the number of modes that make the system response at that

frequency, and the peaks of the first singular value will be equivalent to the natural frequencies of the system.

3 Comparison and Validation

For validating the present research method, the presented natural frequencies are compared with the previous works. Three different geometry have been used for comparison (a square sheet, a rectangular sheet, and a CGS with a circular hole). The achieved frequencies were compared with those obtained by solution based on the nonlocal vibration analysis of a plate based on the first-order shear deformation theory (FSDT) [39, 40] for all three geometries.

3.1 Square Sheet

Since there was a solution for the square sheet, a single-layer square graphene sheet (with dimensions of 2.5×2.5 nm) was simulated by the proposed approach. The natural frequency of a single-layer square graphene sheet, extracted from the work of Pradhan et al. [39] and Jalali et al. [40] is presented in Table 1.

3.2 Rectangular Plate

The numerical results of Pradhan et al. [39] and Jalali et al. [40] for rectangular graphene sheet with dimensions of 2.5×5 nm have also been listed in Table 1.

Table 1 The fundamental natural frequency of the square and rectangular graphene sheet in the non-local mode under the simply-supported boundary condition

Size (nm)	Non-local Parameter	ω (THz)	Reference
2.5×2.5	0	0.9970	Jalali et al. [40]
	1	0.4893	
	0	1.0062	Pradhan et al. [39]
	1	0.4934	
2.55622×2.53000	—	**0.4834**	**MD (present)**
2.5×0.5	0	0.6359	Jalali et al. [40]
	1	0.3688	
	0	0.6385	Pradhan et al. [39]
	1	0.3703	
2.51385×5.23300		**0.3687**	**MD (present)**

Table 2 The first natural frequency of a CGS with a concentric circular hole under SS boundary conditions

Boundary Condition	$\omega(1,1)$ (THz)	Reference
Simply Support (SS)	0.5384519	M. Mohammadi et al. [41]
	0.5371094	MD (present)

Table 3 The natural frequencies (THz) of a defect-free CGS with $R_1 = 20$Å

Boundary Condition	Mode Number			
Simply Support (SS)	1	2	3	4
	0.03394	0.05347	0.06299	0.08203

3.3 Defective Circular Sheet

To confirm the natural frequencies of defective sheets, a CGS with a radius of 40 Å with a concentric hole in the center has been considered so that the radius of the inner circle to the radius of the outer circle was to 0.4. Notably, both of the inner and the outer circles were simply-supported. The numerical results reported by Mohammadi et al. [41] Considering the non-local theory has been presented in Table 2. It could be seen that the obtained result was well suited to the values which were reported by Mohammadi et al. [41].

4 Results and Discussion

The analysis of nanomaterials is important due to their numerous applications. Considering the limitations of experimental methods in the investigation of nanoscale materials, the development of theoretical approaches and atomic simulations will be highly valuable. In this respect, the molecular dynamics simulation has attracted many researchers' attention as an efficient technique that is capable of predicting the experimental results. In this study, the effects of CGS geometry and hole boundary conditions on the natural frequency of holed CGSs have been investigated. The sheets' natural frequencies were obtained for the first to fourth modes using different hole eccentricities and diameters under SS and FS boundary conditions.

Table 3 shows the first four frequencies of a pristine CGS with simply-supported edges.

Tables 4 and 5 show the first four frequencies of CGSs with a hole with different boundary conditions.

According to the results in Tables 4 and 5, it is evident that the changes in boundary conditions and the geometry of CGSs influenced notably their

Table 4   The natural frequencies (THz) of the first four modes of a CGS with $R_1 = 20$ Å with a circular hole defect in free boundary condition for circular defect

Boundary Condition	a	R_2/R_1	1st Mode	2nd Mode	3rd Mode	4th Mode
FS	**0**	0.1	0.03662	0.05737	0.06372	0.08304
		0.15	0.03599	0.04983	0.05908	0.08012
		0.2	0.03516	0.04956	0.05737	0.07861
		0.25	0.03215	0.04911	0.05732	0.07632
		0.3	0.03198	0.04901	0.05724	0.07514
		0.35	0.03154	0.04852	0.05719	0.07320
		0.4	0.03076	0.0481	0.05713	0.07104
	0.1	0.1	0.03613	0.05273	0.06909	0.07959
		0.15	0.03581	0.05184	0.06847	0.07784
		0.2	0.03557	0.0498	0.05762	0.07617
		0.25	0.03551	0.04925	0.05622	0.07415
		0.3	0.03199	0.04902	0.05437	0.07326
		0.35	0.03125	0.04896	0.05216	0.06949
		0.4	0.03101	0.04834	0.05029	0.06641
	0.2	0.1	0.03613	0.05469	0.06689	0.07739
		0.15	0.03601	0.05143	0.05671	0.07592
		0.2	0.03491	0.05103	0.05518	0.07568
		0.25	0.03259	0.05075	0.05467	0.07502
		0.3	0.03194	0.04943	0.05395	0.07211
		0.35	0.03138	0.04872	0.05306	0.07068
		0.4	0.03125	0.04834	0.05127	0.06641
Pristine Sheet under SS	0		0.03394	0.05347	0.06299	0.08203

natural frequency. In all the examined cases, the outer circle radius was fixed. The inner-circle (hole) radius was considered as 2, 4 and 8 Å. As observed in Table 4, the obtained natural frequencies do not have similar trends under FS and SS boundary conditions.

In order to evaluate the role of defects, the absolute frequency shift (FSR) was defined as Δf (change in frequency when a defect was made in the CGS) and the frequency shift ratio (FSR) as $\gamma = |\Delta f|/f_{\text{pristine}}$.

Frequency shift ratios were plotted for various boundary conditions and geometries. In the following, $a = e/R_1$ and $r = R_2/R_1$ are the eccentricity

Table 5 The natural frequencies (THz) of the first four modes of a CGS with $R_1 = 20$ Å with a circular hole defect in simply support boundary condition for circular defect

Boundary Condition	a	R_2/R_1	1st Mode	2nd Mode	3rd Mode	4th Mode
SS	**0**	0.1	0.05664	0.0647	0.06543	0.08204
		0.15	0.05912	0.06659	0.07852	0.08526
		0.2	0.06714	0.06763	0.07910	0.08813
		0.25	0.06825	0.07312	0.08146	0.08962
		0.3	0.07236	0.07748	0.08632	0.09783
		0.35	0.08262	0.08218	0.08917	0.09914
		0.4	0.10280	0.10520	0.10820	0.12450
	0.1	0.1	0.05566	0.05762	0.06177	0.07617
		0.15	0.05781	0.06042	0.06917	0.08122
		0.2	0.05908	0.0752	0.07739	0.08423
		0.25	0.06128	0.07853	0.07893	0.08953
		0.3	0.06335	0.07913	0.08464	0.09042
		0.35	0.06944	0.08159	0.08847	0.09125
		0.4	0.08340	0.09155	0.09424	0.09790
	0.2	0.1	0.03296	0.04785	0.06006	0.07910
		0.15	0.04432	0.05967	0.07158	0.08714
		0.2	0.05249	0.06274	0.07617	0.08887
		0.25	0.05526	0.06545	0.0796	0.09012
		0.3	0.05983	0.06938	0.08159	0.09254
		0.35	0.06145	0.07252	0.09025	0.09620
		0.4	0.06396	0.07544	0.09399	0.11040
Pristine Sheet under SS	0		0.03394	0.05347	0.06299	0.08203

and radius ratios, respectively. Figure 5 depicts the variations of frequency shift concerning the eccentricity and radius ratios for the FS boundary condition of a defective CGS.

As seen in Figure 5, the FSR of circular holed CGS under the FS boundary condition increased with the radius ratio increase. Except for the first and the second modes, higher eccentricity ratios led to a higher level of FSR. For the first and the second modes, change in FSR was approximately independent of the eccentricity ratio. Then, spacing the center of the hole from the center of the CGS did not affect the FSR much for the first and the second modes.
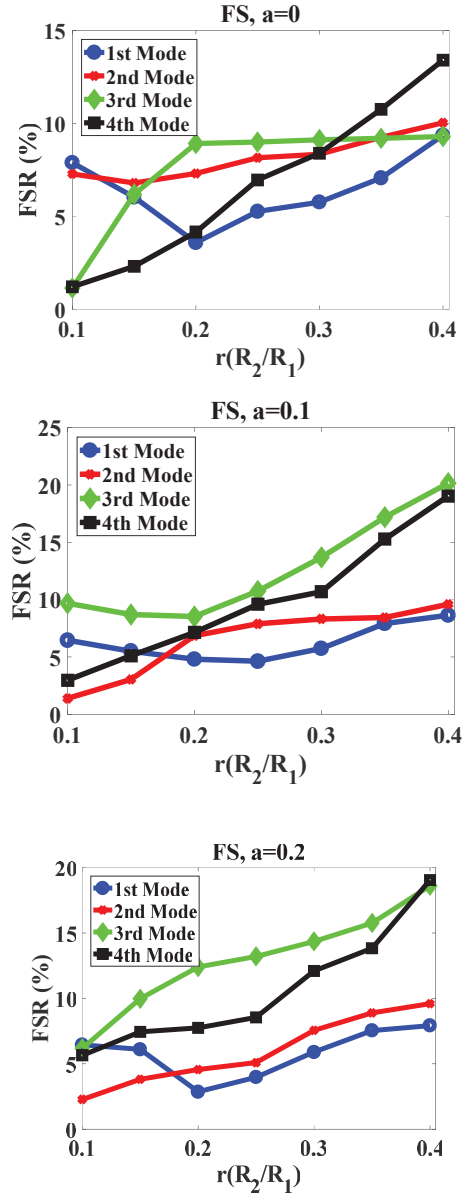
Figure 5 Variation of frequency shift ratio (FSR) concerning the eccentricity and radius ratios for free-simply supported boundary condition (FS) of a CGS with an eccentric hole. (a) a = 0, (b) a = 0.1 and (c) a = 0.2.
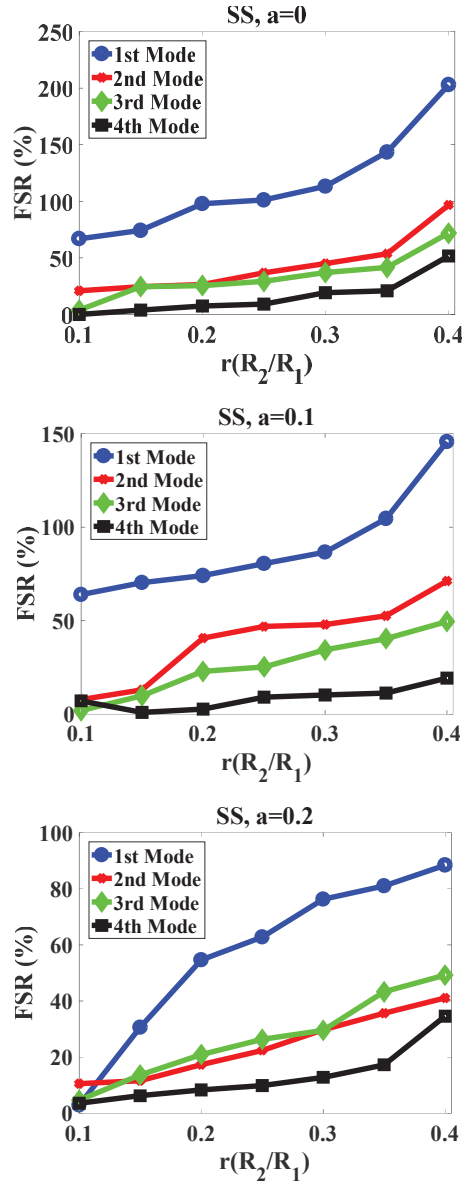
Figure 6   Variation of frequency shift ratio (FSR) concerning the eccentricity and radius ratios for simply-supported boundary condition (SS) of a CGS with an eccentric hole. (a) a = 0, (b) a = 0.1 and (c) a = 0.2.

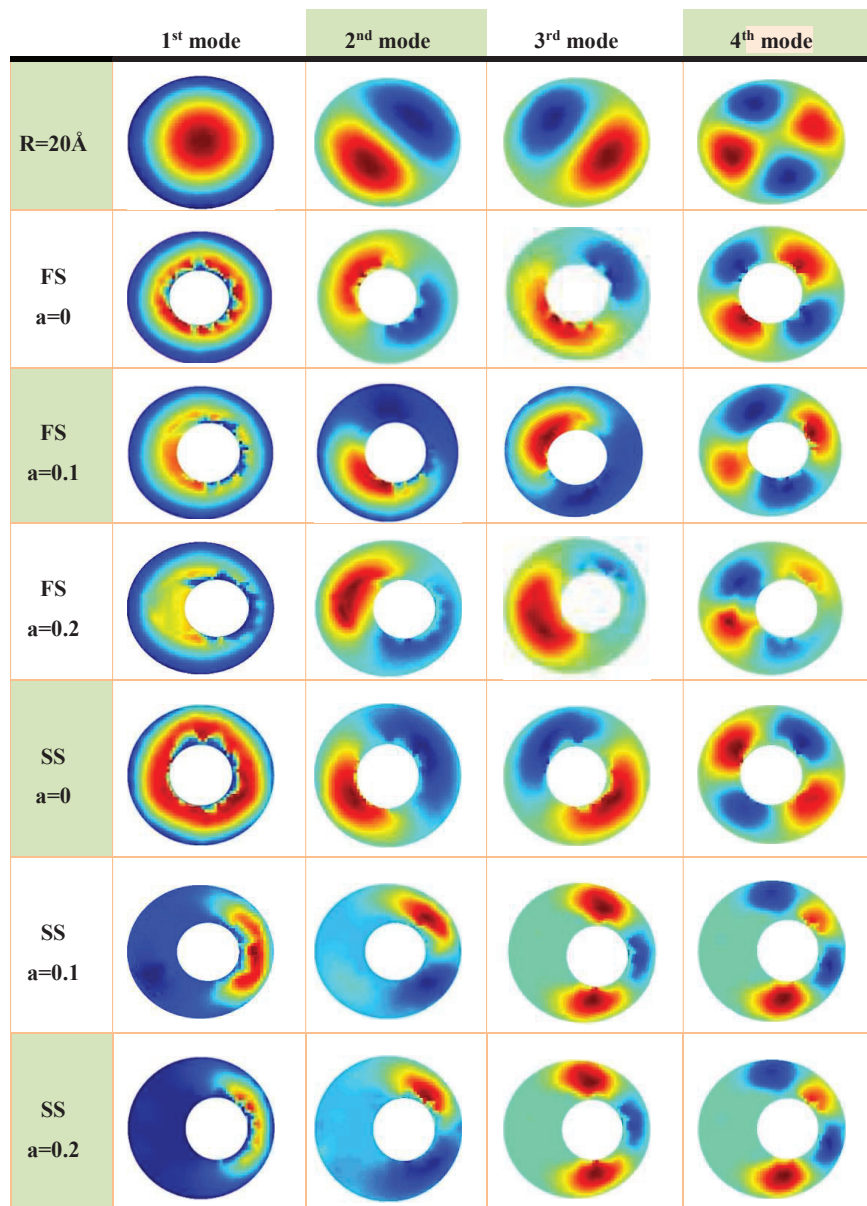|	1st mode	2nd mode	3rd mode	4th mode
R=20Å				
FS a=0				
FS a=0.1				
FS a=0.2				
SS a=0				
SS a=0.1				
SS a=0.2				

Figure 7 Comparison the first four mode shapes of a pristine and defected graphene sheet with various eccentric distance for both boundary conditions.

Figure 6 shows the variation of frequency shift ratio (FSR) concerning the eccentricity and radius ratios for a CGS with an eccentric hole under a simply-supported boundary condition (SS).

From Figure 6, the FSR of circular holed CGS under SS boundary condition considerably increased with the increase in the radius ratio. Unlike the FS boundary condition, the FSR level was very large in the SS boundary condition. The first mode experienced the most changes with increasing the radius ratio and decreasing the eccentricity ratio.

Comparison of Figures 5 and 6 demonstrated that the sensitivity of the frequency of a holed CGS was considerable when the sheet was under SS boundary condition. In that state, the larger hole size and lower eccentricity increased the sensitivity more than before. Then, when a hole is inevitable, drawing out the hole from the center of the sheet and performing FS boundaries led to less sensitivity.

In order to better evaluation of the effect of boundary condition and eccentricity on the vibrational behavior of CGS, the mode shapes are presented in Figure 7.

As shown in Figure 7, when the hole was placed at the center of the sheet (e = 0), the mode shapes were the same as the pristine sheet. Increasing the eccentricity leads to a considerable difference from the pristine mode shapes. The center of the deflection of mode shapes was always in the center of the hole. It showed that one could displace the extremum of displacement from the CGS center.

5 Conclusion

In this paper, the effects of a circular hole of different sizes in a single-layer CGS on its natural frequency using molecular dynamics simulation was studied. Also, by the first time, the effects of eccentric hole on the vibrational behavior of a single-layer CGS using molecular dynamics approach has been investigated.

The comparison between the natural frequencies of defect-free and holed CGSs obtained by molecular dynamics simulation has revealed the following results:

1. For computing the natural frequency values and observing the vibration behavior of CGSs in various modes, the molecular dynamics simulation method could be used with a good approximation instead of numerical and analytical solutions.

2. In the case of free boundary conditions for the hole, the natural frequency of a holed CGS normally diminished with the hole size increase in all the considered modes.
3. When the hole's interior boundary was supported, the natural frequency of a holed CGS normally increased with the increase in the hole size in all the examined modes.
4. Under the SS boundary condition, the natural frequency of a holed CGS (when the hole and circular graphene were concentric) was more than that of a defect-free sheet, which was obvious, considering the existence of a hole.
5. With the increase of hole eccentricity, the natural frequency of holed CGS diminished under SS/FS boundary condition.
6. The absolute frequency shift (FSR) of circular holed graphene sheets under the FS boundary condition increased with the radius ratio increase. Except for the first and the second modes, higher eccentricity ratios lead to a higher level of change in FSR. For the first and the second modes, change in FSR was approximately independent of the eccentricity ratio. Affected, spacing the center of the hole from the graphene sheet's center did not affect the frequency shift much.
7. The FSR of circular holed graphene sheets under SS boundary condition considerably increased with the radius ratio increase. Unlike the FS boundary condition, the FSR level was very large in the SS boundary condition. With the increase of the eccentricity ratio diminished FSR. The first mode experienced the most changes with increasing the radius ratio and decreasing the eccentricity ratio.
8. Generally, the sensitivity of the frequency of a holed graphene sheet was considerable when the sheet was under SS boundary condition. In that state, larger hole size and lower eccentricity increased the sensitivity more than before. Then, when a hole was inevitable, drawing out the hole from the center of the sheet and also performing FS boundaries lead to less sensitivity.

Eventually future works planned for improvement the subject are:

1. Structural changes of circularly defected multi-layer circular graphene Nanosheets upon mechanical vibrations.
2. Structural changes of square defected on monolayer and multilayer circular graphene Nanosheets upon mechanical vibrations.
3. Detection of nano particles using a circular graphene sheet with circular and square defects

4. Investigation of thermal treatment in circular graphene sheets with circular defects.

References

[1] M. J. Allen, V. C. Tung, and R. B. Kaner, "Honeycomb carbon: a review of graphene," *Chem. Rev.*, vol. 110, no. 1, pp. 132–145, 2010.

[2] D. R. Dreyer, R. S. Ruoff, and C. W. Bielawski, *Angew. Chemie Int. Ed.*, vol. 49, no. 49, pp. 9336–9344, 2010.

[3] M. J. Allen and V. C. Tung, and R. B. Kaner, Honeycomb carbon: a review of graphene, *Chemical Reviews*, 110, 1, 132–145, 2010. ACS Publicatio.

[4] A. K. Geim and K. S. Novoselov, "The rise of graphene," in *Nanoscience and Technology: A Collection of Reviews from Nature Journals*, World Scientific, 2010, pp. 11–19.

[5] S. Sadeghzadeh and M. M. Khatibi, "Modal identification of single layer graphene nano sheets from ambient responses using frequency domain decomposition," *Eur. J. Mech.*, vol. 65, pp. 70–78, 2017.

[6] C. I. L. Justino, A. R. Gomes, A. C. Freitas, A. C. Duarte, and T. A. P. Rocha-Santos, "Graphene based sensors and biosensors," *TrAC Trends Anal. Chem.*, vol. 91, pp. 53–66, 2017.

[7] H. Tian et al., "Scalable fabrication of high-performance and flexible graphene strain sensors," *Nanoscale*, vol. 6, no. 2, pp. 699–705, 2014.

[8] C. Soldano, A. Mahmood, and E. Dujardin, "Production, properties and potential of graphene," *Carbon N. Y.*, vol. 48, no. 8, pp. 2127–2150, 2010.

[9] Y. Dan, Y. Lu, N. J. Kybert, Z. Luo, and A. T. C. Johnson, "Intrinsic response of graphene vapor sensors," *Nano Lett.*, vol. 9, no. 4, pp. 1472–1475, 2009.

[10] V. Singh, D. Joung, L. Zhai, S. Das, S. I. Khondaker, and S. Seal, "Graphene based materials: Past, present and future," *Prog. Mater. Sci.*, vol. 56, no. 8, pp. 1178–1271, 2011.

[11] X. Wang and G. Shi, "An introduction to the chemistry of graphene," *Phys. Chem. Chem. Phys.*, vol. 17, no. 43, pp. 28484–28504, 2015.

[12] T. Murmu and S. C. Pradhan, "Vibration analysis of nano-single-layered graphene sheets embedded in elastic medium based on nonlocal elasticity theory," *J. Appl. Phys.*, vol. 105, no. 6, p. 64319, 2009.

[13] S. C. Pradhan and J. K. Phadikar, "Small scale effect on vibration of embedded multilayered graphene sheets based on nonlocal continuum models," *Phys. Lett. A*, vol. 373, no. 11, pp. 1062–1069, 2009.

[14] S. A. Fazelzadeh and S. Pouresmaeeli, "Thermo-mechanical vibration of double-orthotropic nanoplates surrounded by elastic medium," *J. Therm. Stress.*, vol. 36, no. 3, pp. 225–238, 2013.

[15] B. Arash and Q. Wang, "Vibration of single-and double-layered graphene sheets," *J. Nanotechnol. Eng. Med.*, vol. 2, no. 1, p. 11012, 2011.

[16] S. R. Asemi and A. Farajpour, "Decoupling the nonlocal elasticity equations for thermo-mechanical vibration of circular graphene sheets including surface effects," *Phys. E Low-dimensional Syst. Nanostructures*, vol. 60, pp. 80–90, 2014.

[17] M. Miri and M. Fadaee, "Effects of eccentric circular perforation on thermal vibration of circular graphene sheets using translational addition theorem," *Int. J. Mech. Sci.* , vol. 100, pp. 237–249, 2015.

[18] S. Hosseini-Hashemi, M. Derakhshani, and M. Fadaee, "An accurate mathematical study on the free vibration of stepped thickness circular/annular Mindlin functionally graded plates," *Appl. Math. Model.*, vol. 37, no. 6, pp. 4147–4164, 2013.

[19] S. R. Asemi, A. Farajpour, M. Borghei, and A. H. Hassani, "Thermal effects on the stability of circular graphene sheets via nonlocal continuum mechanics," *Lat. Am. J. Solids Struct.*, vol. 11, no. 4, pp. 704–724, 2014.

[20] M. Neek-Amal and F. M. Peeters, "Buckled circular monolayer graphene: a graphene nano-bowl," *J. Phys. Condens. Matter*, vol. 23, no. 4, p. 45002, 2010.

[21] Q. H. Wang, K. Kalantar-Zadeh, A. Kis, J. N. Coleman, and M. S. Strano, "Electronics and optoelectronics of two-dimensional transition metal dichalcogenides," *Nat. Nanotechnol.*, vol. 7, no. 11, p. 699, 2012.

[22] S. K. Jalali, M. J. Beigrezaee, and N. M. Pugno, "Atomistic evaluation of the stress concentration factor of graphene sheets having circular holes," *Phys. E Low-dimensional Syst. Nanostructures*, vol. 93, pp. 318–323, 2017.

[23] M. Mirakhory, M. M. Khatibi, and S. Sadeghzadeh, "Vibration analysis of defected and pristine triangular single-layer graphene nanosheets," *Curr. Appl. Phys.*, vol. 18, no. 11, pp. 1327–1337, 2018.

[24] S. H. Madani, M. H. Sabour, and M. Fadaee, "Molecular dynamics simulation of vibrational behavior of annular graphene sheet: Identification

of nonlocal parameter," *J. Mol. Graph. Model.*, vol. 79, pp. 264–272, 2018.

[25] J. Tersoff, "Erratum: Modeling solid-state chemistry: Interatomic potentials for multicomponent systems," *Phys. Rev. B*, vol. 41, no. 5, p. 3248, 1990.

[26] L. Li, M. Xu, W. Song, A. Ovcharenko, G. Zhang, and D. Jia, "The effect of empirical potential functions on modeling of amorphous carbon using molecular dynamics method," *Appl. Surf. Sci.*, vol. 286, pp. 287–297, 2013.

[27] J. R. Walton, L. A. Rivera-Rivera, R. R. Lucchese, and J. W. Bevan, "Morse, Lennard-Jones, and Kratzer potentials: A canonical perspective with applications," *J. Phys. Chem. A*, vol. 120, no. 42, pp. 8347–8359, 2016.

[28] K. Laasonen, A. Pasquarello, R. Car, C. Lee, and D. Vanderbilt, "Car-Parrinello molecular dynamics with Vanderbilt ultrasoft pseudopotentials," *Phys. Rev. B*, vol. 47, no. 16, p. 10142, 1993.

[29] T. J. Martinez, M. Ben-Nun, and R. D. Levine, "Multi-electronic-state molecular dynamics: A. *J. Phys. Chem.*, vol. 100, no. 19, pp. 7884–7895, 1996.

[30] G. Rajasekaran, R. Kumar, and A. Parashar, "Tersoff potential with improved accuracy for simulating graphene in molecular dynamics environment," *Mater. Res. Express*, vol. 3, no. 3, p. 35011, 2016.

[31] G. P. Zhang and Z. G. Wang, "Fatigue of small-scale metal materials: from micro-to nano-scale," in *Multiscale fatigue crack initiation and propagation of engineering materials: structural integrity and microstructural worthiness*, Springer, 2008, pp. 275–326.

[32] F. Shimizu, S. Ogata, and J. Li, "Theory of shear banding in metallic glasses and molecular dynamics calculations," *Mater. Trans.*, p. 710160231, 2007.

[33] X. Xia, G. J. Weng, J. Xiao, and W. Wen, "Porosity-dependent percolation threshold and frequency-dependent electrical properties for highly aligned graphene-polymer nanocomposite foams," *Mater. Today Commun.*, vol. 22, p. 100853, 2020.

[34] "index @ lammps.sandia.gov.".

[35] A. Brandt, *Noise and vibration analysis: signal analysis and experimental procedures*. John Wiley & Sons, 2011.

[36] L. Zhang and R. Brincker, "An overview of operational modal analysis: major development and issues," in *1st international operational modal analysis conference*, 2005, pp. 179–190.

[37] H. Wenzel, "Ambient vibration monitoring," *Encycl. Struct. Heal. Monit.*, 2009.

[38] R. Brincker, L. Zhang, and P. Andersen, "Modal identification of output-only systems using frequency domain decomposition," *Smart Mater. Struct.*, vol. 10, no. 3, p. 441, 2001.

[39] R. Brincker, L. Zhang, and P. Andersen, "Modal identification from ambient responses using frequency domain decomposition," in *Proc. of the 18th International Modal Analysis Conference (IMAC), San Antonio, Texas*, 2000.

[40] S. C. Pradhan and J. K. Phadikar, "Nonlocal elasticity theory for vibration of nanoplates," *J. Sound Vib.*, vol. 325, no. 1–2, pp. 206–223, 2009.

[41] S. K. Jalali, M. H. Naei, and N. M. Pugno, "Graphene-based resonant sensors for detection of ultra-fine nanoparticles: molecular dynamics and nonlocal elasticity investigations," Nano, vol. 10, no. 02, p. 1550024, 2015.

[42] M. Mohammadi, M. Ghayour, and A. Farajpour, "Free transverse vibration analysis of circular and annular graphene sheets with various boundary conditions using the nonlocal continuum plate model," *Compos. Part B Eng.*, vol. 45, no. 1, pp. 32–42, 2013.

Biographies

M. Farzannasab received her B.Sc. degree in mechanical engineering from Semnan University, Semnan, Iran; and then, the M.Sc. degree in mechanical engineering, from K.N. Toosi University of Technology, Tehran, Iran in 2020.

Her fields of interests are in Neural Network,Biomechanics, Bio-Nano-Mechanics, Machine Learning, Control and Machine Design and Robotics (Surgical Robots, Rehabilitation Robots and Human-Robot Interactions). She has research experience in Modal Analysis Laboratory and Mechatronics Mechanism Laboratory for four years.

M. M. Khatibi received B.Sc. and M.Sc. degrees and then, the Ph.D. degree in mechanical engineering from Semnan University, Semnan, Iran. Now, He is an Assistant Professor of department of Solid Design and Applied Design at faculty of mechanical engineering in the Semnan University, Semnan, Iran.

S. Sadeghzadeh received B.Sc. and M.Sc. degrees in mechanical engineering from Semnan University, Semnan, Iran and Iran University of Science and Technology, Tehran, Iran, respectively, and then, the Ph.D. degree Iran University of Science and Technology, Tehran, Iran. His fields of interests are in Experimental Works on NanoRobotics, Robotic, Micro and NanoRobotic, Micro and Nano Manipulators Dynamics and control, Piezoactuating and Molecular and MultiScale Modeling of NanoStructures. His current researches are about Micro and Nano manipulation, Perturbation Compensation, Nonlinearities Avoidance and MultiScale Modeling. Now he is an associate professor in the Iran University of Science and Technology, Tehran, Iran.